Theor Chem Acc (2005) 113: 161–166
DOI 10.1007/s00214-004-0620-1

REGULAR ARTICLE

Nilesh R. Dhumal · Ashwini V. Todkary
Sandhya Y. Rane · Shridhar P. Gejji

Hydrogen bonding motif in 2-hydroxy-1,4-naphthoquinone

Received: 29 August 2004 / Accepted: 15 October 2004 / Published online: 29 January 2005

Abstract Self-assemblies of 2-hydroxy-1,4-naphthoquinone (HNQ) have been investigated using the $(HNQ)_n$ (n =1–4) series as modeled systems employing *ab initio* Hartree–Fock calculations. The energetics and charge distribution in these molecular systems are presented. As revealed from the electron density in the highest occupied molecular orbital of the lowest energy conformers of $(HNQ)_n$ (n =1–4) the charge 'percolates' to the end unit of the assembly. This has been supported by the molecular electrostatic potential topography.

Keywords H-bonding · Charge percolation · Lawsone · Hartree-Fock

1 Introduction

2-hydroxy-1,4-naphthoquinone (HNQ or lawsone) has been of great interest for quite a long time partly due to its biological importance, which stems from its selective action to target a limited number of proteins at the plasma membrane [1]. HNQ can be reduced reversibly to a semiquinone radical anion or to dianionic catecholate form, and on coordination with metal ions such as copper or manganese facilitates electron transfer in photosynthesis and biological processes [2–4]. Thus HNQ has been considered as an electron transfer mediator in biochemical fuel cells [5]. It has also been a novel probe for hydrogen bond donor ability in pure solvents and mixed aqueous solvents [6]. In order to understand the properties from isolated molecules, the electronic structure of HNQ was obtained by using *ab initio* quantum chemical calculations. Its infrared spectral characteristics observed in N_2 and Ar matrices have also been studied extensively [7]. Furthermore, Dekkers [8] has studied the hydrogen bonding interactions in the crystal structure of HNQ. In the present work we carry out detailed investigation of self-assemblies of HNQ by employing the *ab initio* Hartree–Fock (HF) method on the modeled $(HNQ)_n$, where n =1–4, systems, which are facilitated *via* intermolecular hydrogen bonded interactions. To pursue this in the present work we address the following questions: How does the intermolecular hydrogen bonding influence the structural parameters of $(HNQ)_n$? What are the consequences of such hydrogen bonding pertaining to the vibrational frequencies of the modeled $(HNQ)_n$ systems? How does the charge distribution in terms of the topography of the molecular electrostatic potential (MESP) and the electron density in the highest occupied molecular orbital (HOMO) vary along this series? How does the charge distribution influence the dipole moment and the 'energy-gap' of the frontier orbital? The computational method is outlined below.

N. R. Dhumal (✉), A. V. Todkary, S. Y.Rane
Department of Chemistry,
University of Pune, 411007,
India

S. P. Gejji
E-mail: pgejji@chem.unipune.ernet.in

2 Computational method

Ab initio HF optimizations were carried out using the GAUSSIAN 94 program [9] with the internally stored 6-31G(d, p) basis set. The vibrational frequencies were computed using the analytical gradient method. The vibrational frequencies of $(HNQ)_n$ (with n = 1–3) conformers were calculated. Normal vibrations were assigned by visualizing the displacements of atoms around their equilibrium (mean) positions [10]. The localization of the electron density in the HOMO obtained from the Hartree–Fock wavefunction was visualized by employing the UNIVIS-2000 code [10].

The MESP V($\mathbf{r}$), at a point $\mathbf{r}$ due to a molecular system with nuclear charges $\{Z_A\}$ located at $\{\mathbf{R}_A\}$ and electron density $\rho(\mathbf{r})$ is defined by

$$V(\mathbf{r}) = \sum_{A=1}^{N} \frac{Z_A}{|\mathbf{r} - \mathbf{R}_A|} - \int \frac{\rho(\mathbf{r}')d^3\mathbf{r}'}{|\mathbf{r} - \mathbf{r}'|}, \quad (1)$$

where N is the total number of nuclei in the molecule. Thus $V(\mathbf{r})$ comprises of the bare of the bare nuclear potential and the electronic contributions. As can be seen, the balance of these terms (cf. Eq. (1)) brings about the effective localization of electron-rich regions in the molecular system. The $V(\mathbf{r})$

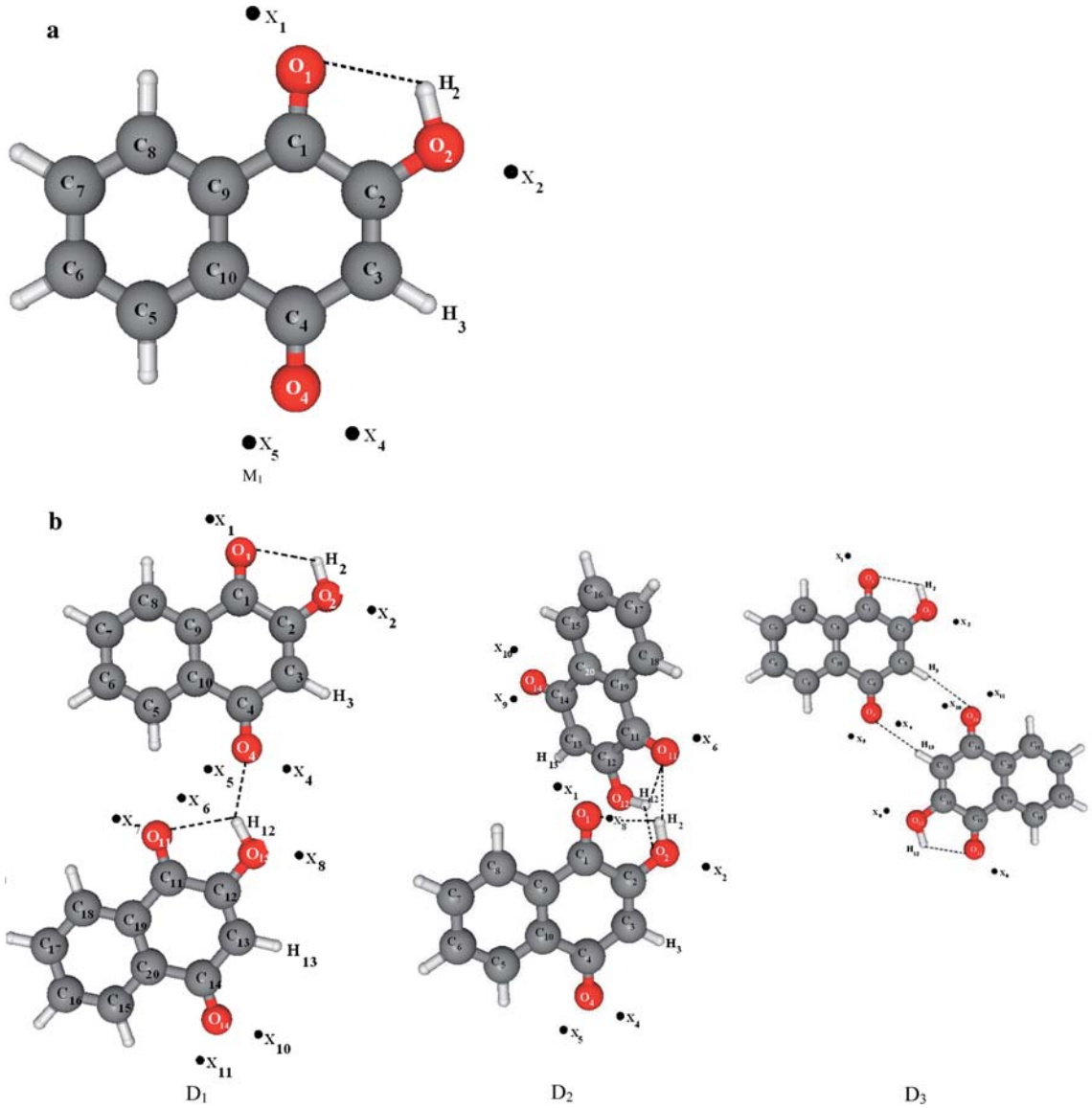

Fig. 1a–d. Optimized geometries of $(HNQ)_n$ (n =1–4) conformers. MESP minima near oxygens are denoted by x_1, x_2, ...

was calculated using the HF wave function and its topographical features [11–14] were studied. The MESP critical points (CPs), where the first-order partial derivatives of a function with respect to all its dependent variables become zero, were located. A non-degenerate CP is characterized by an ordered pair (R, σ), R denoting the rank and σ the signature, the former being the number of non-zero eigenvalues at the CP whereas the latter gives the excess of the positive eigenvalues over the corresponding negative ones. These MESP CPs are classified as maxima, minima and the saddles in terms of R and σ. Thus, (3, −3), (3, −1), (3, +1) and (3, +3) CPs have been identified. Thus (3, +3) CP represents a local minimum in the $V(\mathbf{r})$. For the (3, −3) CP all three eigenvalues of the Hessian matrix are negative, and such a CP corresponds to a local maximum of the MESP. The saddle points are denoted by (3, −1) and (3, +1).

3 Results and discussion

As noted in the introduction we have investigated self-assemblies of $(HNQ)_n$ (n =1–4) as modeled systems. For n =2, 3 and 4 different conformations denoted by D, T, and Te, respectively, were considered. The suffix 1, 2 and 3 represents the mode of intermolecular hydrogen bonding. These are shown in Fig. 1a–d. The intermolecular hydrogen bonding has been facilitated via: (a) oxygen from the C=O group interacting with the hydroxyl group of another unit (as in D_1, T_1 and Te_1); (b) secondly an initial structure for a $(HNQ)_2$ representing π–π interactions has been considered. This structure finally converges to non-planar conformer with flipping of the naphthalene ring (D_2). The two naphthalene rings turn out to be nearly perpendicular to each other in D_2, implying the absence of stacking interactions in the gas phase structure. This

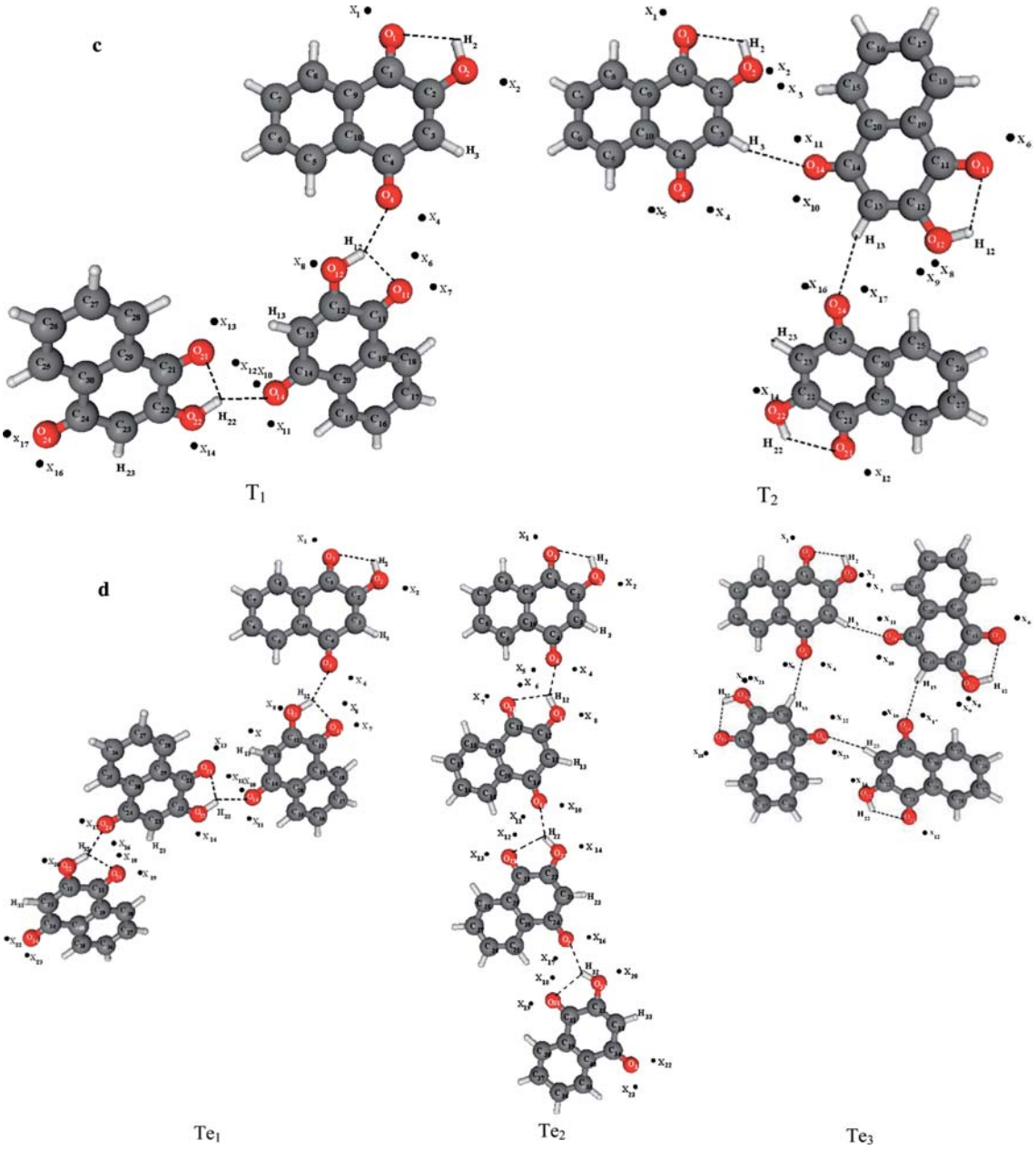

Fig. 1 (Contd).

agrees with the conclusions drawn by Dekkers [8]; (c) lastly a conformer where the hydrogen bonding via C_3-hydrogen of one unit binds to free carbonyl oxygen of the preceding unit is considered. The pattern of such C–H$\cdots$O contacts, which vary with the angle between the carbonyls in some of related naphthoquinones, are investigated extensively in the literature [15]. For $n = 2$ and 4, three conformations corresponding to the stationary point geometries were located. HF/6-31G (d, p) calculations predict the intramolecular $O_1 \cdots H_2$ hydrogen bond distance in isolated (HNQ) to be 2.084 Å.

Amongst the three conformers of $(HNQ)_2$, D_1turns out to be 4.67 kJ mol^{-1} lower in energy than D_2. In the latter,

Table 1 Electronic (in au) and relative stabilization energies (in kJ mol^{-1}) in $(HNQ)_n$ conformers

	SCF energies	Relative stabilization energy
M_1	−606.788173	
D_1	−1213.583863	0.0
D_2	−1213.582084	4.7
D_3	−1213.581133	7.2
T_1	−1820.380370	0.0
T_2	−1820.370407	26.2
Te_1	−2427.177395	0.0
Te_2	−2427.175852	4.1
Te_3	−2427.164396	34.1

Table 2 Inter- and intramolecular hydrogen bond distances in different $(HNQ)_n$ conformers

	M_1	D_1	D_2	D_3	T_1	T_2	Te_1	Te_2	Te_3
$R(O_1 \cdots H_2)$	2.084	2.084	2.146	2.082	2.085	2.082	2.086	2.085	2.061
$R(O_{11} \cdots H_{12})$		2.217	2.146	2.082	2.186	2.064	2.188	2.219	2.061
$R(O_4 \cdots H_{12})$		2.048			2.046		2.039	2.031	
$R(O_{11} \cdots H_2)$			2.232						
$R(O_2 \cdots H_{12})$			2.391						
$R(O_{21} \cdots H_{22})$					2.227	2.063	2.225	2.226	2.061
$R(O_{14} \cdots H_{22})$					1.992		1.987	2.016	
$R(O_{31} \cdots H_{32})$							2.223	2.226	2.061
$R(O_{24} \cdots H_{32})$							1.992	2.027	
$R(O_4 \cdots H_{13})$				2.487		2.480			2.513
$R(O_{14} \cdots H_3)$				2.487					
$R(O_{14} \cdots H_{23})$						2.480			2.513
$R(O_{34} \cdots H_{23})$									2.513
$R(O_4 \cdots H_{33})$									2.513

two naphthalene rings are oriented at 96° to one another. The D_3 structure is further destabilized by 2.5 kJ mol^{-1} (cf. Table 1). Both D_1 and D_2 exhibit bifurcated hydrogen bonds through the hydroxyl H_{12} in D_1 and both H_2 and H_{12} in D_2, as shown in Fig. 1b. The inter- and intramolecular hydrogen bond distances in all these structures are displayed in Table 2. The intermolecular $O_4 \cdots H_{12}$ distance in D_1 is 2.084 Å. The $O_{11} \cdots H_2$ (2.232 Å) and $O_2 \cdots H_{12}$ (2.391 Å) bonds are unequal in the non-planar D_2 conformer. The intermolecular bond distance in D_1 is 2.048 Åcompared to 2.232 Å ($O_{11} \cdots H_2$) and 2.391 Å($O_2 \cdots H_{12}$) in D_2, which provides stability to the D_1 conformer of $(HNQ)_2$. In conformer D_3 neither of the carbonyls participate in the propagation of self-assemblies. The possibility of helical structure has been predicted for D_1 and D_2 conformers. In the former, O$\cdots$H interactions are stronger and the asymmetric charge distributions near O_{11} and O_2 are noticed.

For $n = 3$, two conformers T_1 and T_2 are shown in Fig. 1c, of which the conformer T_1 with a pair of bifurcated hydrogen bonds (inter- and intramolecular as well) turns out to be 26.2 kJ mol^{-1} lower in energy. The stability of T_1 relative to T_2 results from the strong O–H$\cdots$O interactions over the C–H$\cdots$O interactions and is in accordance with the bond distances displayed in Table 1. Thus, the lowest energy T_1 conformer shows half-helical structure. It should be remarked here that, as noted earlier in D_3, the T_2 conformer prohibits further extension of the HNQ assemblies. In the case of $(HNQ)_4$, the structures Te_1 and Te_2, possessing three bifurcated hydrogen bonds through different centers, were derived by considering $(HNQ)_3 \cdots (HNQ)$ and $(HNQ)_2 \cdots (HNQ)_2$ interactions. For $(HNQ)_4$, conformer Te_1 turns out to be lower in energy by 4.04 kJ mol^{-1} than Te_2 owing to stronger $O_{14} \cdots H_{22}$ and $O_{24} \cdots H_{32}$ interactions. The structure including solely (HNQ)$\cdots$(HNQ) interactions finally converges to a structure with C_4 symmetry (denoted by Te_3 in Fig. 1d), with all carbonyl oxygens prohibiting further propagation of the self-assemblies, and is destabilized by 34.1 kJ mol^{-1} over Te_1 (cf. Table 1). In Table 3 the interaction energies, ΔE, obtained by subtracting the sum of electronic energies of the individual fragment from the total self-consistent field (SCF) electronic energy of the $(HNQ)_n$, are displayed. Thus

Table 3 Interaction energies (ΔE) in kJ mol^{-1} in $(HNQ)_n$ conformers

	ΔE
D_1	19.74
D_2	15.07
D_3	12.57
T_1	41.62
T_2	15.46
Te_1	23.24
Te_2	21.34
Te_3	30.73

$(HNQ)_3$ is favored over the $n = 2$ and $n = 4$, which suggests $(HNQ)_3$ as a basic unit in a crystal.

The charge distribution in $(HNQ)_n$ has been investigated using the MESP topography. MESP minima near oxygens in different conformers of $(HNQ)_n$ (n = 1–4) are given in Table 4. In the lowest energy conformers (M_1, D_1, T_1, Te_1), increasing value of n engenders shallow MESP minima near O_1 and O_2. On the other hand the carbonyl oxygen in propagation of assembly show deeper MESP minima, which implies 'percolation of electronic charge' to the end unit. The $O_4 \cdots H_{13}$ and $O_{14} \cdots H_3$ hydrogen bonds in D_3 are equal (2.487 Å) and engender the electrostatic potential, which is symmetric (O_4, O_{14} and O_2, O_{12} are, therefore, symmetry equivalent). Carbonyl oxygens in D_3 prohibit extension of self-assembly. Similarly carbonyl oxygens in T_2 are locked in intra- and intermolecular hydrogen bonded interactions facilitating no further propagation of assembly, in contrast to T_1. Similar conclusions may be drawn from the electrostatic potentials of $(HNQ)_4$ conformers.

The HOMO (isosurface of 0.01 au) in the lowest energy conformers of $(HNQ)_n$ (n =1–4), viz., M_1, D_1, T_1 and Te_1, are displayed in Fig. 2. It should be remarked here that the percolation of charge (via O–H$\cdots$O hydrogen bonded interactions) has been noticed only in the lowest energy $(HNQ)_n$ conformers. This charge transport via O–H$\cdots$O intermolecular interactions is revealed from the electron density within the HOMO and is consistent with the conclusion drawn from the MESP topography.

Table 4 MESP minima (in kJ mol^{-1}) near oxygen atoms of different $(HNQ)_n$ conformers

	Nearest atom	M_1	D_1	D_2	D_3	T_1	T_2	Te_1	Te_2	Te_3
x_1	O_1	−146.2	−138.4	−141.2	−158.1	−133.1	−159.4	−130.5	−134.0	−161.8
x_2	O_2	−150.2	−141.3	−146.5	−180.8	−136.0	−139.4	−133.5	−137.3	−126.2
x_3	O_2						−139.0			−189.2
x_4	O_4	−196.9	−125.5	−219.9	−201.7	−189.8	−256.2	−187.3	−176.0	−148.6
x_5	O_4	−220.5	−184.6	−197.2	−168.8		−215.4		−118.3	−251.9
x_6	O_{11}		−111.9	−133.2	−158.1	−164.1	−159.7	−168.4	−103.1	−161.8
x_7	O_{11}		−131.8			−172.3		−159.7	−121.2	
x_8	O_{12}		−194.6	−150.5	−180.8	−160.7	−138.1	−156.8	−182.6	−126.2
x_9	O_{12}						−138.0			−148.8
x_{10}	O_{14}		−213.5	−218.3	−201.7	−100.6	−244.6	− 93.8	−196.1	−189.2
x_{11}	O_{14}		−239.7	−195.1	−168.8	−185.4	−185.3	−178.7	−137.7	−251.9
x_{12}	O_{21}					−130.2	−156.3	−121.4	−117.9	−161.8
x_{13}	O_{21}					−150.2		−140.9	−131.4	
x_{14}	O_{22}					−202.7	−164.4	−195.9	−194.5	−148.6
x_{15}	O_{22}									
x_{16}	O_{24}					−220.8	−230.4	−110.0	−208.3	−189.2
x_{17}	O_{24}					−247.1	−177.8	−192.1	−147.8	−251.9
x_{18}	O_{31}							−163.9	−142.6	−161.9
x_{19}	O_{31}							−141.5	−128.6	−126.2
x_{20}	O_{32}							−209.5	−207.5	
x_{21}	O_{32}									−148.6
x_{22}	O_{34}							−253.9	−221.6	−189.2
x_{23}	O_{34}							−228.2	−248.4	−251.9

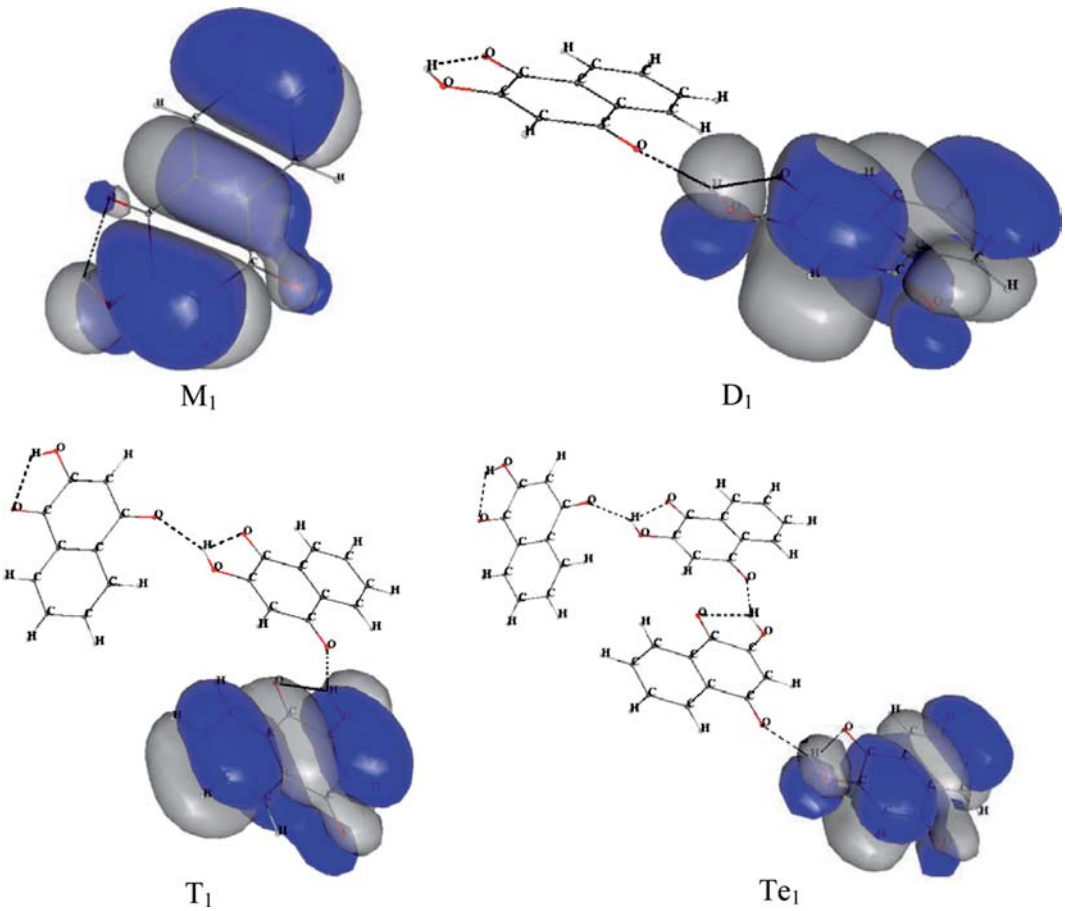

Fig. 2 Highest occupied molecular orbital (HOMO) in the lowest energy conformers (M_1, D_1, T_1 and Te_1) of modeled $(HNQ)_n$ (n =1–4) systems. The isosurface of 0.01 au are shown. See text for details

Table 5 Highest occupied molecular orbital (HOMO) to lowest unoccupied molecular orbital (LUMO) energy gap, ($\Delta\varepsilon$), (in kJ mol^{-1}) and dipole moments, μ, (in D) in $(HNQ)_n$ conformers

	$\Delta\varepsilon$	μ
M_1	1,006	3.31
D_1	964	6.61
D_2	996	4.77
D_3	999	0.00
T_1	948	5.50
T_2	996	2.06
Te_1	934	8.47
Te_2	948	13.15
Te_3	1,001	0.00

Table 6 Comparison of selected vibrational frequencies (in cm^{-1}) of the lowest energy $(HNQ)_n$ conformers

Assignment	M_1	D_1	T_1
O-H[a] stretching		3,474 (919)	3,428 (1,335)
C=O[b] stretching	1710 (41)	1,709 (15)	1,717 (105)
C=O[c] stretching	1697 (619)	1,688 (1,302)	1,677 (1,213)

[a] The OH vibration corresponds to the unit participating in further propagations
[b] Oxygen locked in the intermolecular hydrogen bonded interactions
[c] Oxygen participating in further propagations via C=O$\cdots$H interactions

The energy difference of the frontier orbitals ($\Delta\varepsilon$) and the dipole moments of $(HNQ)_n$ conformers are given in Table 5. Thus it may be inferred that the conformer of lowest energy is soft relative to those of higher energy and becomes more so with increasing n along the $(HNQ)_n$ series. The dipole moments do not show any regular trend. As expected the D_3 and Te_3 conformers have zero dipole moments owing to a symmetric charge distribution (cf. Fig. 1b 1d).

The vibrational frequencies of selected normal vibrations in $(HNQ)_n$ (n = 1–3), are compared in Table 6. HF/6-31G(d, p) calculated frequencies were scaled by a factor 0.8606 since the observed C=O stretching for the isolated HNQ corresponds to 1,710 cm^{-1}. The carbonyl oxygen locked with the hydroxyl group, via O_2–$H_2\cdots O_1$ hydrogen bonded interactions, engenders a five-membered ring. This leads to C=O stretching at a 1,710 cm^{-1} vibration for HNQ. In the $(HNQ)_2$ this vibration moves to a lower wavenumber and a shift of 9 cm^{-1} has been predicted. A red shift of 20 cm^{-1} has been predicted for T_3. The corresponding C=O and OH bond distances are nearly unchanged in the M_1, D_1 and T_1 conformers. The 1,717 cm^{-1} vibration suggests that the C=O bond participating in propagation of self-assembly in T_1 is relatively strong. This is accompanied with an increase of intensity, possibly resulting from the electron-rich carbonyl oxygen, which brings about charge separation to a larger extent in T_1.

4 Conclusions

As shown in this work the geometrical parameters of isolated HNQ, except the intermolecular hydrogen bond distances, are nearly insensitive along the $(HNQ)_n$ (n =1–4) series. The work demonstrates how the charge transfers from the top to the top to the end along the half-helix in the $(HNQ)_n$ modeled systems. This has been manifested in the deeper MESP minima near carbonyl oxygens with the growth of HNQ self-assembly. The electron densities within the HOMO and the MESP topography support these conclusions. The energy gap of Frontier orbitals decreases steadily along the $(HNQ)_n$ series.

Acknowledgements SPG and NRD acknowledge support from the Council of Scientific and Industrial Research [Project 01(1772)/02/EMR–II], New Delhi, India. Thanks are due to C–DAC, Pune, for providing the computational facilities. AVT is thankful to the Bhabha Atomic Research Centre (BARC) for providing research fellowship through the Pune University–BARC collaborative program.

References

1. Odile M, Dreyer J (1994) Biochem J 300:99
2. Allakhverdiev SI, Karacan MS, Somer G, Karcan N, Khan EM, Rane SY, Padhye S, Kilmov VV, Renger G (1994) Biochem 33:12210
3. Thomson RH (1971) Naturally occurring quinones. Academic, New York
4. Morton RA (1965) Biochemistry of quinones. Academic, New York
5. Tanaka K, Tamamushi R, Ogawa T (1985) J Technol Biotech 35B:191
6. Idriss KA, Sadaira H, Hashem EY, Saleh MS, Soliman SA (1996) Monatshefte fuer Chemie 127:29
7. Rostkowska H, Nowak MJ, Lapinski L, Adamowicz L (1998) Spectrochim. Acta A 54:1091
8. Dekkers J, Kooijman H, Kroon J, Grech E (1996) Acta Cryst C 52:2896
9. GAUSSIAN94 package: Frisch MJ, Trucks GW, Schlegel HB, Gill PMW, Johnson BG, Robb MA, Cheeseman JR, Keith T, Peterson GA, Montgomery JA, Raghavachari K, Al–laham MA, Zakrzewski VG, Oritz JV, Forseman JB, Cioslowski J, Stefanov BB, Nanayakkara A, Challacombe M, Peng CY, Ayala PY, Chen W, Wong MW, Andres JL, Replolge ES, Gomperts R, Martin RL, Fox DJ, Binkley JS, Defrees DJ, Baker J, Stewart JJP, Head–Gordon M, Gonzalez C, Pople JA (1995) GAUSSIAN Inc., Pittusburgh
10. Limaye AC, Gadre SR (2001) Curr Sci 80:1298
11. Gadre SR, Shrisat RN (2000) Electrostatics of atoms and molecules. Universites Press, Hyderabad, and references therein
12. Naray-Szabo G, Ferenczy GG (1995) Chem Rev 95:829
13. Pingale SS, Gadre SR, Bartolotti LJ (1998) J Phys Chem A 102:9987
14. Gadre SR, Kulkarni SA, Shivastava IA (1992) J Chem Phys 96:5253
15. Patai S, Rappoport Z (1988) The Chemistry of quinonoid compounds, Part 1, vol. 2. Wiley, Berlin Heidelberg New York, p. 87